Electronic Raman scattering in double semi-parabolic quantum wells*

N. Zamani, A. Keshavarz†, and M. J. Karimi

Department of Physics, College of Sciences, Shiraz University of Technology, P.O. Box 313-71555, Shiraz, Iran

(Received 8 October 2012; revised manuscript received 26 November 2012)

The differential cross-section for electronic Raman scattering in double semi-parabolic quantum wells of typical GaAs/$Al_xGa_{1-x}As$ is investigated numerically with the effective-mass approximation. The dependence of the differential cross-section on structural parameters such as the barrier width and the well widths is studied. Our results indicate that the electronic Raman scattering is affected by the geometrical size and can be negligible in the symmetric double-well case.

Keywords: electronic Raman scattering, double semi-parabolic quantum wells

PACS: 78.30.–j, 78.67.–n, 78.67.Ch, 78.20.Bh **DOI:** 10.1088/1674-1056/22/5/057802

1. Introduction

It is well known that the evolution of molecular-beam epitaxy combined with the use of the modulation doping technique has made it possible to fabricate new nanometric structures, such as quantum dots, quantum wires, and quantum wells. Studies on these new structures open a new field in fundamental physics and chemistry. Some attention has been focused on their applications in nanophotonic devices.[1–5] It is very important to know the electronic and the optical properties of these structures for the optoelectronic device design. However, few theoretical analyses of the electronic and optical properties associated with the intersubband optical transitions in these structures are presented in scientific literature.[6–9] Specifically, the nanostructure double quantum well is very interesting as far as the device industry is concerned, and is widely used because it offers the possibility to create an artificial three-level system. Double quantum well (DQW) semiconductor heterostructures are suitable candidates for technological applications such as Raman lasers[10,11] and quantum cascade lasers,[12] as they are suitable candidates for novel application of electron devices.[13–15]

The electronic Raman scattering (ERS) is known as a useful tool to obtain direct information on the energy band structure and the optical properties in low-dimensional semiconductor systems.[16,17] The electronic structures of nanostructures and other materials can be studied by using the Raman scattering processes considering different polarizations of incident and emitted radiations.[18–20] The differential cross-section in general shows singularities related to the interband and the intraband transitions. Recently, the ERS in low-dimensional semiconductor systems has been the subject of many theoretical and experimental investigations.[21–26] In all previous works, the Schrödinger equation was solved analytically to find the energy eigenvalues and the corresponding wave functions, then the results were used to obtain the optical properties of nanostructures. However, there is no analytical solution of the Schrödinger equation for many finite quantum well systems. Progress in computational physics with high accuracy permits us to investigate new QW and DQW nanostructures. The double semi-parabolic quantum well (DSPQW) potential was used in a quantum well laser.[27] For the first time, we investigated the linear and the nonlinear optical absorptions and the refractive index changes of the DSPQW potential.[28] In this paper, we study the ERS of the DSPQW potential, which is shown schematically in Fig. 1, where an electron in the conduction band of the first well undergoes an intersubband transition to a new energy level of the same well, absorbing a photon of energy $\hbar\omega_l$ (pump radiation); after that, the electron emits a photon of energy $\hbar\omega_s$ (laser radiation) and undergoes an intersubband transition to the last quantum well.[29,30] The numerical methods are employed to solve the Schrödinger equation for the DSPQW, which consists of two different width GaAs wells coupled with a thin $Al_xGa_{1-x}As$ barrier.

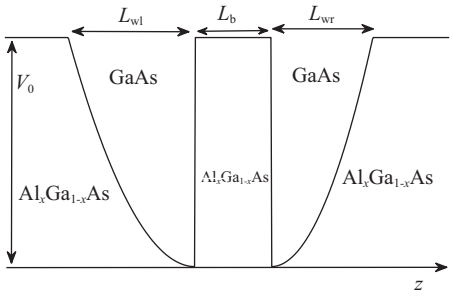


Fig. 1. Schematic diagram for DSPQW with well widths L_{wl} and L_{wr} and barrier width L_b.

The outline of the paper is as follows. In Section 2, we

*Project supported by the Shiraz University of Technology, Iran.

†Corresponding author. E-mail: Keshavarz@sutech.ac.ir

© 2013 Chinese Physical Society and IOP Publishing Ltd

review and summarize the formalism of the ERS of the system. Section 3 is allocated to the numerical calculation for the energy eigenvalues and the eigenfunctions of electrons in the DSQW. We also investigate the behavior of the ERS for the DSPQW in this section. The conclusions are given in Section 4.

2. Theory

2.1. Electronic state

Consider one-dimensional time-independent Schrödinger equation of an electron in the DSPQW within the framework of effective mass approximation

$$-\frac{\hbar^2}{2m^*}\left(\frac{\mathrm{d}^2}{\mathrm{d}z^2}+V(z)\right)\psi(z)=E\psi(z), \tag{1}$$

where m^* is the constant effective mass, and $V(z)$ is the one-dimensional confinement potential profile of the DSPQW depicted in Fig. 1, which is[28]

$$V(z)=\begin{cases}\dfrac{1}{2}m^*\omega_{\mathrm{l}}^2\left(z+\dfrac{L_{\mathrm{b}}}{2}\right)^2, & -\dfrac{L_{\mathrm{b}}}{2}-L_{\mathrm{wl}}<z<-\dfrac{L_{\mathrm{b}}}{2},\\ V_0, \quad |z|\le\dfrac{L_{\mathrm{b}}}{2}, & z\ge\dfrac{L_{\mathrm{b}}}{2}+L_{\mathrm{wr}}, \quad z\le-\dfrac{L_{\mathrm{b}}}{2}-L_{\mathrm{wl}},\\ \dfrac{1}{2}m^*\omega_{\mathrm{r}}^2\left(z-\dfrac{L_{\mathrm{b}}}{2}\right)^2, & \dfrac{L_{\mathrm{b}}}{2}<z<\dfrac{L_{\mathrm{b}}}{2}+L_{\mathrm{wr}}.\end{cases} \tag{2}$$

The origin of the growth direction z is taken to be the center of the structure. This structure consists of two GaAs well layers with widths L_{wl} and L_{wr}, respectively, separated by an undoped $\mathrm{Al}_x\mathrm{Ga}_{1-x}\mathrm{As}$ barrier layer with width L_{b}, and the frequencies of the semi-parabolic confinement potentials of the left and the right wells are ω_{l} and ω_{r}, respectively. Here $V_0=Q_c\Delta E_{\mathrm{g}}$, where Q_c is the band offset ratio, and ΔE_{g} is the band-edge discontinuity between GaAs and $\mathrm{Al}_x\mathrm{Ga}_{1-x}\mathrm{As}$. The Schrödinger equation with this potential profile cannot be solved analytically, so the numerical calculation is needed. Therefore, we use the fourth-order Runge–Kutta method to calculate the direct numerical solutions to obtain the energy levels and the corresponding wave functions for electrons in the conduction band of DSPQW. Notice that the solutions of the envelope function approximation must satisfy the boundary conditions, i.e., both $\psi(z)$ and the current $\partial\psi(z)/\partial z m^*$ must be continuous. Note that the wave functions obtained from this numerical solution are not normalized, but the normalization can be easily achieved with the following transformation:

$$\psi(z)\to\frac{\psi(z)}{\sqrt{\int_{-\infty}^{\infty}\psi^*(z)\psi(z)}}. \tag{3}$$

Results of the above formalism can be used to calculate the electronic Raman scattering introduced in the following section.

2.2. Electronic Raman scattering

The differential cross-section (DCS) per unit solid angle for electronic Raman scattering in volume V for incoming light of frequency ω_{l} and scattered light of frequency ω_{s} is given by[31]

$$\frac{\mathrm{d}^2\sigma}{\mathrm{d}\omega_{\mathrm{s}}\,\mathrm{d}\Omega}=\frac{V^2\omega_{\mathrm{s}}^2 n(\omega_{\mathrm{s}})}{8\pi^3c^4n(\omega_{\mathrm{l}})}W(\omega_{\mathrm{s}},\boldsymbol{e}_{\mathrm{s}}), \tag{4}$$

where $n(\omega)$ is the refractive index as a function of the radiation frequency, $\boldsymbol{e}_{\mathrm{s}}$ ($\boldsymbol{e}_{\mathrm{l}}$) is the unit polarization vector for the emitted secondary (incoming) radiation, c is the speed of light in a vacuum, and $W(\omega_{\mathrm{s}},\boldsymbol{e}_{\mathrm{s}})$ is the transition rate for the emission of the secondary radiation (with frequency ω_{s} and polarization $\boldsymbol{e}_{\mathrm{s}}$) introduced according to Fermi's golden rule

$$W(\omega_{\mathrm{s}},\boldsymbol{e}_{\mathrm{s}})=\frac{2\pi}{\hbar}\sum_f|M_f|\delta(E_f-E_i). \tag{5}$$

Here

$$|M_f|=\sum_a\frac{\langle f|\hat{H}_{\mathrm{s}}|a\rangle\langle a|\hat{H}_{\mathrm{l}}|i\rangle}{(E_i-E_a+\mathrm{i}\Gamma_a)}$$

is the scattering amplitude probability of the Raman process, and $\delta(E_f-E_i)=\Gamma_f/[\pi(E_f-E_i)^2+\Gamma_f^2]$. States $|i\rangle$, $|a\rangle$, and $|f\rangle$ represent the initial, the intermediate, and the final states of the system with their corresponding energies E_i, E_a, and E_f, while Γ_a and Γ_f are the lifetime broadenings in the intermediate and the final states, respectively. The Hamiltonian corresponding to frequency ω_{r} of the radiation field is given by

$$\hat{H}_{\mathrm{r}}=\frac{|e|}{m^*}\sqrt{\frac{2\pi\hbar}{V\omega_{\mathrm{r}}}}(\boldsymbol{e}_{\mathrm{r}}\cdot\hat{\boldsymbol{p}}), \tag{6}$$

where $\hat{\boldsymbol{p}}=-\mathrm{i}\hbar\nabla$ and $r=l(s)$ describe the interaction between the electron and the incident (secondary) radiation field in the dipole approximation.[32–35] The effect of the reduced dimensionality on the free carrier absorption has been calculated, the selection rules for intraband and intersubband are shown in Ref. [36]. Therefore equation (6) is rewritten as

$$\hat{H}_{\mathrm{r}}=-\mathrm{i}\hbar(\boldsymbol{e}_{\mathrm{r}}\cdot\boldsymbol{e}_{\mathrm{s}})\frac{|e|}{m^*}\sqrt{\frac{2\pi\hbar}{V\omega_{\mathrm{r}}}}\frac{\partial}{\partial z}. \tag{7}$$

Hence, for the incident and the secondary radiations, transitions due to emission or absorption of light occur only if the polarization vectors of radiations coincide to the $\boldsymbol{e}_z$ transition.

In the initial state, we have an electron in the conduction band and an incident photon. The initial state energy is given by $E_i=E_{ni}+\hbar\omega_{\mathrm{l}}$. In the final state, we have a secondary radiation photon and an electron. The final state energy can be written as $E_f=E_{nf}+\hbar\omega_{\mathrm{s}}$. As the electron absorbs the incident photon or the electron emits the secondary photon of energy $\hbar\omega_{\mathrm{s}}$, the energy conservation law results in

$$E_i-E_a=E_{nf}-E_{na}+\hbar\omega_{\mathrm{s}}, \tag{8}$$

$$E_i-E_f=\hbar\omega_{\mathrm{l}}-\hbar\omega_{\mathrm{s}}+E_{ni}-E_{nf}. \tag{9}$$

In order to calculate the differential cross-section from Eq. (4), we should calculate the matrix elements in Eq. (5). For the case of the radiation field, by using Eq. (7), the matrix elements of the intraband transitions of the intermediate state in the conduction band can be written as[37]

$$\begin{aligned}\langle\psi_a|\hat{H}_{\rm r}|\psi_{\rm b}\rangle &= \langle\psi_a| - {\rm i}\hbar(\boldsymbol{e}_{\rm r}\cdot\boldsymbol{e}_z)\frac{|e|}{m^*}\sqrt{\frac{2\pi\hbar}{V\omega_{\rm r}}}\frac{\partial}{\partial z}|\psi_{\rm b}\rangle \\ &= -{\rm i}\hbar(\boldsymbol{e}_{\rm r}\cdot\boldsymbol{e}_z)\frac{|e|}{m^*}\sqrt{\frac{2\pi\hbar}{V\omega_{\rm r}}}T_{a,b}(i), \qquad (10)\end{aligned}$$

where

$$T_{a,b}(i) = d_{\rm r}\left(\beta_1\langle\psi_a^{\rm out}|\frac{\partial}{\partial z}|\psi_{\rm b}^{\rm out}\rangle + \beta_2\langle\psi_a^{\rm in}|\frac{\partial}{\partial z}|\psi_{\rm b}^{\rm in}\rangle\right),$$

with

$$\beta_{1(2)} = \frac{m_0^*}{m_{1(2)}^*}, \quad \frac{1}{m_0^*} = \frac{1}{m_1^*} + \frac{1}{m_2^*},$$

and

$$\frac{1}{d_{\rm r}} = \sum_i \frac{1}{d_i}.$$

By substituting Eqs. (8) and (10) into Eq. (4), the differential cross-section for a three-level system ($E_i = E_1$, $E_f = E_3$, $E_a = E_2$) is calculated for a DSPQW and expressed in the form

$$\left[\frac{{\rm d}^2\sigma}{{\rm d}\Omega\,{\rm d}\omega_{\rm s}}\right]_i = \sigma_0\frac{\omega_{\rm s}}{\omega_{\rm l}}|M_0(i)|^2\frac{E_0^2}{[\hbar\omega_{\rm l} - \hbar\omega_{\rm s} + E_1 - E_2]^2 + \Gamma_f^2}, \qquad (11)$$

where

$$M_0(i) = E_0\frac{T_{2,3}(i)T_{3,1}(i)}{\hbar\omega_{\rm s} + E_2 - E_3 + {\rm i}\Gamma_a},$$

$$\sigma_0 = \frac{4e^4 n(\omega_{\rm s})\hbar\Gamma_f}{\pi m_0^{*2}c^4 n(\omega_{\rm l})E_0^2}|(\boldsymbol{e}_{\rm l}\cdot\boldsymbol{e}_z)(\boldsymbol{e}_{\rm s}\cdot\boldsymbol{e}_z)|^2,$$

and

$$E_0 = \frac{\hbar^2}{2m_0^* d_{\rm r}^2}.$$

Eventually, we calculate the scattering efficiency for the emission spectrum of the electronic Raman laser scattering process, in which two singularities can be observed when $\hbar\omega \to \hbar\omega_{\rm s} = E_3 - E_2$ and $\hbar\omega \to {\rm SL} = \hbar\omega_{\rm l} + E_1 - E_2$ (SL: step-like) corresponding to the resonant and the non-resonant peaks, respectively. We should note that the resonant peak does not depend on the incoming radiation while the non-resonant peak depends on it.

3. Numerical results and discussion

In this section, the DCS is calculated numerically for the typical semiconductor $Al_xGa_{1-x}As$/GaAs DSPQW. For this purpose, the energy eigenvalues and the corresponding wave functions are numerically calculated. The wave functions of the DSPQW are plotted in Fig. 2 for (a) the symmetric case with $L_{\rm wl} = L_{\rm wr} = 10$ nm and $L_{\rm b} = 6$ nm, and (b) the asymmetric case with $L_{\rm wl} = 10$ nm, $L_{\rm wr} = 8$ nm, and $L_{\rm b} = 6$ nm.

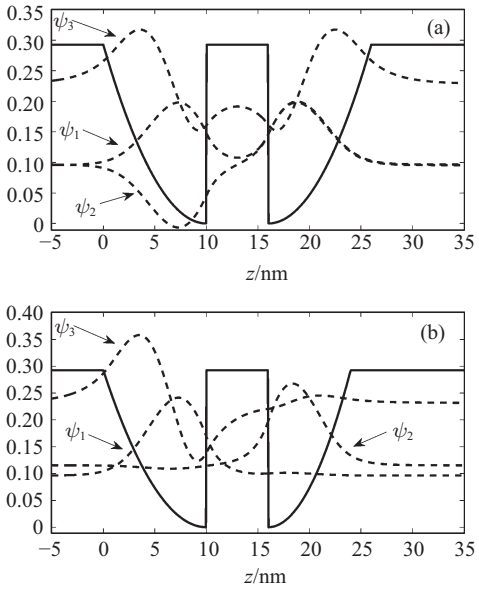


Fig. 2. Schematic diagram of the DSPQW and wave functions for (a) symmetrical case with $L_{\rm wl} = L_{\rm wr} = 10$ nm and $L_{\rm b} = 6$ nm, and (b) asymmetrical case with $L_{\rm wl} = 10$ nm, $L_{\rm wr} = 8$ nm, and $L_{\rm b} = 6$ nm.

The other physical parameters used in this paper are as follows: $m^*_{\rm GaAs} = 0.067m_{\rm e}$, $m^*_{\rm AlGaAs} = (0.067 + 0.083x)m_{\rm e}$ ($m_{\rm e}$ is the rest mass of electron), $\Delta E_{\rm g} = 1.247x$ (x is the mole fractional of Al), incident radiation energy $\hbar\omega_{\rm l} = 0.23$ eV, and the lifetimes of the final and intermediate states $\Gamma_f = \Gamma_a = 3$ meV. Figure 3 displays the Raman spectra as a function of secondary radiation photon energy $\hbar\omega_{\rm s}$ with different widths of the barrier ($L_{\rm b} = 2, 4, 6$ nm). In Fig. 3(a), a symmetric $Al_xGa_{1-x}As$/GaAs DSPQW with well widths $L_{\rm wl} = L_{\rm wr} = 10$ nm is used; in Fig. 3(b), an asymmetric $Al_xGa_{1-x}As$/GaAs DSPQW with well widths $L_{\rm wl} = 10$ nm and $L_{\rm wr} = 8$ nm is used. From Figs. 3(a) and 3(b), we can observe that with the increasing thickness of the barrier, the resonant and the non-resonant peaks decrease and shift to higher energies. The comparison between Figs. 3(a) and 3(b) shows that two peaks in the asymmetrical case of DSPQW are bigger than those in the symmetrical case. However, the peaks of resonant and non-resonant in the symmetric case have a more distinct blue shift than that in the asymmetric case.

Figure 4 shows the Raman laser cross-section versus the secondary radiation photon energy $\hbar\omega_{\rm s}$ for three different values of the first well width ($L_{\rm wl} = 6, 8, 10$ nm).

The barrier thickness and the second well width are kept at $L_{\rm b} = 6$ nm and $L_{\rm wr} = 8$ nm, respectively. It can be seen that the two peaks of resonant and non-resonant are reduced with the increasing first well width and their displacements have receded from each other. The emission spectra for three different values of the second well width ($L_{\rm wr} = 6, 8, 10$ nm) with fixed first well width $L_{\rm wl} = 8$ nm and barrier width $L_{\rm b} = 6$ nm are calculated as a function of the secondary radiation photon energy $\hbar\omega_{\rm s}$. The obtained results are similar to those in Fig. 4 and show that when the two wells are symmetric, the emission

spectrum disappears.

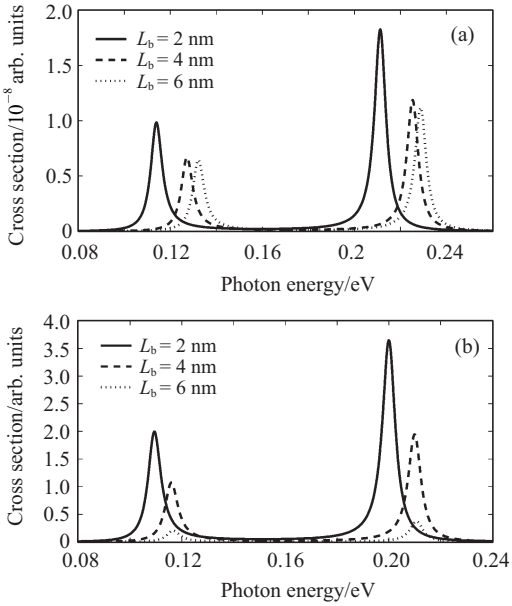


Fig. 3. Raman laser cross-sections for DSPQWs with different widths of the barrier: (a) symmetrical case with $L_{wl} = L_{wr} = 10$ nm, (b) asymmetrical case with $L_{wl} = 10$ nm, $L_{wr} = 8$ nm.

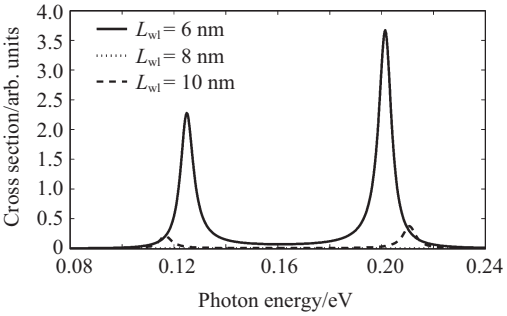


Fig. 4. Emission spectra versus the secondary radiation photon energy for three different values of the first well width.

4. Conclusion

In conclusion, we have investigated the electronic Raman scattering of the DSPQW. The results are presented as functions of the secondary photon energy. The electronic Raman scattering of quantum wells, which depends on the energy eigenstates and the corresponding eigenfunctions, is calculated numerically by solving the Schrödinger equation. It has been shown that the electronic Raman scattering of the DSPQW is strongly affected by the geometrical size and any change in the structure leads to changes in the electronic Raman scattering and the frequency of the secondary radiation. Besides, numerical results show that the peaks of the electronic Raman scattering for the asymmetric structure of the DSPQW are more eminent. By increasing the thickness of the barrier and the well widths, the electron Raman scattering is reduced, and the position of the non-resonant peak shifts to higher energies. These numerical investigations are especially useful for understanding the optical properties of the low-dimensional semiconductor systems.

References

[1] Karabulut I and Baskoutas S 2008 *J. Appl. Phys.* **103** 073512
[2] Liu C H and Xu B R 2008 *Phys. Lett. A* **372** 888
[3] Park S H and Hong W P 2010 *Chin. Phys. Lett.* **27** 098502
[4] Zhu J H, Wang L J, Zhang S M, Wang H, Zhao D G, Zhu J J, Liu Z S, Jiang D S and Yang H 2011 *Chin. Phys. B* **20** 077804
[5] Wang Y B, Xu Y, Yu Z, Yu X, Song G F and Chen L H 2011 *Chin. Phys. B* **20** 067302
[6] Xu P S, Xie C K, Pan H B and Xu F Q 2004 *Chin. Phys.* **13** 2126
[7] Gue D S and Liu B G 2012 *Chin. Phys. B* **21** 017101
[8] Peter J A and Lee C W 2012 *Chin. Phys. B* **21** 087302
[9] Hong W P and Park S H 2011 *Chin. Phys. B* **20** 098502
[10] Maung S M and Katayama S 2004 *Physica E* **21** 774
[11] Miura M and Katayama S 2006 *Sci. Tech. Adv. Mater.* **7** 286
[12] Faist J, Capasso F, Sivco D L, Sirtori C, Hutchinson A L and Cho A Y 1994 *Science* **264** 553
[13] Ohno Y, Matsusue T and Sakaki H 1993 *Appl. Phys. Lett.* **62** 1952 4
[14] Leo K, Shah J, Göbel E O G, Gordon J P and Schmitt-Rink S 1992 *Semicond. Sci. Technol.* **7** B394
[15] Liu L, Swierkowski L, Neilson D and Szymaiski J 1996 *Phys. Rev. B* **53** 7923
[16] Cardona M and Guntherodt G 1989 *Light Scattering in Solids V* (Topics in Applied Physics Vol. 66) (Heidelberg: Springer)
[17] Comas F, Trallero-Giner C and Perez-Alvarez R J 1986 *J. Phys. C: Solid State Phys.* **19** 6479
[18] Cardona M 1990 *Superlatt. Microstruct.* **7** 183
[19] Clein M V 1986 *IEEE J. Quantum Electron.* **22** 1760
[20] Pinczuk A and Burstein 1983 *Light Scattering in Solid I* Vol. 8 (Heidelberg: Springer)
[21] Zhao X F and Liu C H 2007 *Physica E* **36** 34
[22] Lu F and Liu C H 2011 *Superlatt. Microstruct.* **50** 582
[23] Betancourt-Riera R, Riera R and Rosas R 2012 *Physica E* **44** 1152
[24] Liu C H, Ma B K and Chen C Y 2002 *Chin. Phys.* **11** 0730
[25] Liang S J, Xie W F and Lu L L 2011 *Physica B* **406** 652
[26] Xie W F 2012 *Phys. Lett. A* **376** 1657
[27] Verdeyen J T 1995 *Laser Electronics* (3rd edn.) (New Jersey: Prentice-Hall) 475
[28] Keshavarz A and Karimi M J 2010 *Phys. Lett. A* **374** 2675
[29] Khurgin J B, Sun G, Friedman L R and Soref R A 1995 *J. Appl. Phys.* **78** 7398
[30] Sun G, Khurgin J B, Friedman L R and Soref R A 1998 *J. Opt. Soc. Am. B* **15** 648
[31] Comas F, Trallero Giner C and Perez-Alvarez R 1986 *J. Phys. C: Solid State Phys.* **19** 6479
[32] Riera R, Comas F, Trallero-Giner C and Pavlov S T 1988 *Phys. Status Solidi b* **148** 533
[33] Betancourt-Riera R, Riera R, Rosas R and Marín J L 2003 *Phys. Low-Dimens. Struct.* **1–2** 125
[34] Bergues J M, Riera R, Comas F and Trallero-Giner C 1995 *J. Phys.: Condens. Matter* **7** 7273
[35] Bergues J M, Betancourt-Rier R, Rosas R and Marín J L 2000 *J. Phys.: Condens. Matter* **12** 7983
[36] Riera R, Marín J L and Rosas R 2001 *Optical Properties and Impurity States in Nanostructured Materials* (Handbook of Advanced Electronic and Photonic Devices Vol. 6) (New York: Academic) Chap. 6
[37] Betancourt-Riera R, Rosas R , Marín-Enriquez I, Riera R and Marín J L 2005 *J. Phys.: Condens. Matter* **17** 4451